



Fructose-bisphosphate aldolase and enolase from *Echinococcus granulosus*: Genes, expression patterns and protein interactions of two potential moonlighting proteins

Karina Rodrigues Lorenzatto ^a, Karina Mariante Monteiro ^a, Rodolfo Paredes ^c, Gabriela Prado Paludo ^a, Marbella Maria da Fonsêca ^d, Norbel Galanti ^e, Arnaldo Zaha ^{a,b}, Henrique Bunselmeyer Ferreira ^{a,b,*}

^a Laboratório de Genômica Estrutural e Funcional and Laboratório de Biologia Molecular de Cestódeos, Centro de Biotecnologia, Universidade Federal do Rio Grande do Sul (UFRGS), Porto Alegre, RS, Brazil

^b Departamento de Biologia Molecular e Biotecnologia, Instituto de Biociências, UFRGS, Porto Alegre, RS, Brazil

^c Escuela de Medicina Veterinaria, Facultad de Ecología y Recursos Naturales, Universidad Andrés Bello, Santiago, Chile

^d Laboratório Nacional de Computação Científica, Petrópolis, RJ, Brazil

^e Programa de Biología Celular y Molecular, Instituto de Ciencias Biomédicas, Facultad de Medicina, Universidad de Chile, Santiago, Chile

ARTICLE INFO

Article history:

Accepted 17 June 2012

Available online 28 June 2012

Keywords:

Glycolytic enzymes

Moonlighting functions

Cestode

Host–parasite interplay

ABSTRACT

Glycolytic enzymes, such as fructose-bisphosphate aldolase (FBA) and enolase, have been described as complex multifunctional proteins that may perform non-glycolytic moonlighting functions, but little is known about such functions, especially in parasites. We have carried out *in silico* genomic searches in order to identify FBA and enolase coding sequences in *Echinococcus granulosus*, the causative agent of cystic hydatid disease. Four FBA genes and 3 enolase genes were found, and their sequences and exon–intron structures were characterized and compared to those of their orthologs in *Echinococcus multilocularis*, the causative agent of alveolar hydatid disease. To gather evidence of possible non-glycolytic functions, the expression profile of FBA and enolase isoforms detected in the *E. granulosus* pathogenic larval form (hydatid cyst) (EgFBA1 and EgEno1) was assessed. Using specific antibodies, EgFBA1 and EgEno1 were detected in protoscolex and germinal layer cells, as expected, but they were also found in the hydatid fluid, which contains parasite's excretory–secretory (ES) products. Besides, both proteins were found in protoscolex tegument and *in vitro* ES products, further suggesting possible non-glycolytic functions in the host–parasite interface. EgFBA1 modeled 3D structure predicted a F-actin binding site, and the ability of EgFBA1 to bind actin was confirmed experimentally, which was taken as an additional evidence of FBA multifunctionality in *E. granulosus*. Overall, our results represent the first experimental evidences of alternative functions performed by glycolytic enzymes in *E. granulosus* and provide relevant information for the understanding of their roles in host–parasite interplay.

© 2012 Elsevier B.V. Open access under the [Elsevier OA license](http://creativecommons.org/licenses/by/3.0/).

1. Introduction

The larval stage (hydatid cyst or metacestode) of *Echinococcus granulosus* is the causative agent of cystic hydatid disease, a worldwide zoonosis of important medical and economic impacts (Budke et al.,

2006; Moro and Schantz, 2009). The hydatid cyst is the largest parasite structure that lodges within mammalian tissues, and its location and immunogenicity result in a large potential for eliciting inflammation (Siracusano et al., 2008). Nevertheless, the hydatid cyst is able to survive decades in the intermediate host, secreting and exposing molecules that downregulate host responses against the parasite.

The repertoire of known proteins from the hydatid cyst was initially restricted to immunodominant antigens (Carmena et al., 2006; Zhang and McManus, 2006), but, more recently, proteomic surveys have significantly increased the number of *E. granulosus* proteins identified in cyst components (Aziz et al., 2011; Monteiro et al., 2010). Both, in antigen characterization studies and in proteomic surveys, many cytosolic proteins, including glycolytic enzymes, were also consistently found in extracellular host-interacting components (e.g. tegument, and hydatid fluid) (Aziz et al., 2011; Chemale et al., 2003; Monteiro et al., 2010; Rodrigues et al., 1993), and the ectopic presence of these proteins was taken as evidence of potential moonlight functions.

Moonlighting proteins refer to a subset of multifunctional proteins in which two or more different functions are performed by one poly

Abbreviations: cDNA, DNA complementary to RNA; DAPI, 4',6-diamidino-2-phenylindole; EgEno, *E. granulosus* enolase; EgFBA, *E. granulosus* FBA; ELISA, enzyme-linked immunosorbent assay; ES, excretory–secretory products; EST, expressed sequence tag; FBA, fructose-bisphosphate aldolase; Fru 1,6-P₂, fructose 1,6-bisphosphate; GST, glutathione S-transferase; IgG, immunoglobulin G; IPTG, isopropyl β-D-thiogalactopyranoside; LC-MS/MS, liquid chromatography–tandem mass spectrometry; ORF, open reading frame; rEgEno1, recombinant *E. granulosus* enolase isoform 1; rEgFBA1, recombinant *E. granulosus* FBA isoform 1; SDS-PAGE, sodium dodecyl sulfate–polyacrylamide gel electrophoresis; Sulfo-SBED, sulfo-succinimidyl-2-[6-(biotinamido)-2-(p-azido-benzamido) hexanoamido] ethyl-1,3-dithiopropionate; TEV, tobacco etch virus.

* Corresponding author at: Laboratório de Genômica Estrutural e Funcional, Centro de Biotecnologia, UFRGS, Caixa Postal 15005, 91501-970 Porto Alegre, RS, Brazil. Tel.: +55 51 3308 7768; fax: +55 51 3308 7309.

E-mail address: henrique@cbit.ufrgs.br (H.B. Ferreira).

peptide chain (Jeffery, 1999). Many of the currently known moonlighting proteins are highly conserved enzymes, and enzymes involved in sugar metabolism particularly appear to moonlight (Huberts and Van Der Klei, 2010). It has been suggested that at least 7 out of the 10 glycolytic enzymes exhibit various non-glycolytic activities (Sriram et al., 2005), whose functions can vary from structural to regulatory, depending on the organism (Gancedo and Flores, 2008; Starnes et al., 2009).

Fructose-bisphosphate aldolase (FBA), enolase and other glycolytic enzymes have been commonly identified in the tegument and in excretory–secretory (ES) products of various parasites, showing antigenic properties and potential for mediating interactions with the host (Bernal et al., 2004; Huang et al., 2009; Marcilla et al., 2007; McCarthy et al., 2002). In parasites, both FBA and enolase have been described as moonlighting proteins, with involvement in key processes, such as motility, adhesion, invasion, differentiation and development (Jewett and Sibley, 2003; Labbé et al., 2006; Pal-Bhowmick et al., 2007; Pomel et al., 2008). These proteins have the ability to bind host macromolecules, such as plasminogen (Bernal et al., 2004; Marcilla et al., 2007), promoting degradation of extracellular matrix components and favoring the pathogen spread in host tissues (Haile et al., 2006; Nogueira et al., 2010). In helminths, the plasminogen-binding ability appears to contribute to parasite establishment in the host (Marcilla et al., 2007), preventing clot formation around the parasites (Ramajo-Hernández et al., 2007).

Here, we surveyed *Echinococcus* genome and transcriptome databases in order to identify FBA and enolase genes and their encoded isoforms. *E. granulosus* FBA isoform 1 (EgFBA1) and enolase isoform 1 (EgEno1) were cloned and expressed in *Escherichia coli*, and antisera raised against the recombinant proteins were used to determine the expression profile of these enzymes in hydatid cyst components. The EgFBA1 3D structure was modeled and a predicted EgFBA1–actin interaction was experimentally confirmed. Possible moonlighting functions of these enzymes in the host–parasite interplay are discussed.

2. Materials and methods

2.1. Parasite material

E. granulosus hydatid cysts (G1 strain, typed according to Bowles et al., 1992) were obtained from livers and lungs of cattle slaughtered in a local abattoir (Cooperleo, São Leopoldo, Brazil), and individual fertile cysts were processed essentially as described by Monteiro et al. (2010). Animal slaughtering was conducted according to Brazilian laws and under supervision of the *Serviço de Inspeção Federal* (Brazilian Sanitary Authority) of the Brazilian *Ministério da Agricultura, Pecuária e Abastecimento*. Condemned viscera at post-mortem meat inspection due to the presence of hydatid cysts were collected at the abattoir and dissected in the laboratory, following protocols approved by the Ethical Committee of the *Universidade Federal do Rio Grande do Sul* (UFRGS). Protoscoleces were collected by aspiration, washed several times in PBS and treated with pepsin 0.1% in Hanks salt solution pH 2.0 for 15 min to eliminate remnants of the germinal layer and dead protoscoleces.

The protoscolex tegument extract was isolated using a freeze/thawing/vortexing method according to Roberts et al. (1983). The protein extraction was performed essentially as described by Mulvenna et al. (2010b), with the isolated teguments successively washed three times in each of the following buffers and temperatures: (i) 40 mM Tris, pH 7.4 at 4 °C; (ii) 5 M urea in 40 mM Tris, pH 7.4 at room temperature; and (iii) 0.1% SDS, 1% Triton X-100 in 40 mM Tris, pH 7.4 at room temperature.

To obtain excretory–secretory (ES) products, protoscoleces were cultivated similarly as described by Virginio et al. (2012), with some modifications. Protoscoleces were cultured in 4 ml of RPMI medium for 48 h, at 37 °C. The culture supernatant was collected and 10-fold

concentrated using an Amicon Ultra-4 3 kDa MWCO centrifugal filter device (Millipore).

2.2. Nucleotide and amino acid sequence analyses

FBA and enolase expression sequence tag (EST) clusters were obtained from the LophoDB Database (<http://nema.cap.ed.ac.uk/Lopho/LophoDB.php>) (Fernández et al., 2002). Related genomic sequences were recovered from *E. granulosus* and *E. multilocularis* genome data available on Wellcome Trust Sanger Institute (<http://www.sanger.ac.uk/resources/downloads/helminths/echinococcus-granulosus.html>; <http://www.sanger.ac.uk/resources/downloads/helminths/echinococcus-multilocularis.html>) and on GeneDB (Logan-Klumpler et al., 2012; www.genedb.org). Searches for FBA and enolase genes in the available contigs/supercontigs were performed using the *Echinococcus* Blast Server (<http://www.sanger.ac.uk/cgi-bin/blast/submitblast/Echinococcus>). Recovered contigs and scaffolds (referred at Table S1) were submitted to GeneMark-ES (Lomsadze et al., 2005), Fgenesh (Salamov and Solovyev, 2000) and GeneScan (Burge and Karlin, 1998) to determine protein-coding potential and exon–intron gene structure. *In silico* gene predictions were compared to *E. multilocularis* gene-models available on GeneDB (<http://www.genedb.org/Homepage/Emultilocularis>), with *in silico* exon predictions manually adjusted according to *E. multilocularis* gene-models based on RNA evidence.

DNA and protein sequences were aligned using ClustalW2 (Larkin et al., 2007) and Clustal Omega (Sievers et al., 2011), respectively. Alignments were edited using GeneDoc Ver. 2.6.002 (Nicholas and Nicholas, 1997). DNA sequence translations and predictions of protein molecular masses and isoelectric points were performed using tools available on ExPASy website (<http://expasy.org/>).

2.3. RNA extraction, cDNA synthesis and cloning

Total RNA was extracted from *E. granulosus* protoscoleces using the Trizol reagent (Invitrogen). The obtained RNA was treated with DNase I, RNase-free (Fermentas) and reverse transcribed using M-MuLV Reverse Transcriptase (Fermentas) and Oligo(dT)₁₈ Primer (Fermentas). The cDNA synthesis was followed by PCR amplification with High Fidelity DNA Polymerase (Fermentas) using gene-specific primers for EgFBA1 (5′-ATGGCTCGTTTGGTCCCTAC-3′ and 5′-GTAGGCGTGGTTGGCCAC-3′) and EgEno1 (5′-ATGTCCATCTTAAAGATCCA-3′ and 5′-CAAAGGATTGCGGAAGT-3′), which were designed according to EgFBA1 and EgEno1 EST clusters. In the first PCR amplification, 27 nt recombination tags FrecI (5′-TCTGAAAACCTGTATTTTCAGGGAGAA-3′) and RreI (5′-CGCGCGAGGCAGATCGTCAGTCAGTCA-3′), matching pGEX-TEV, were added to the ends of the 5′ and 3′ gene-specific primers, respectively. Secondary PCR amplification was performed using the primary reaction as template and the following primers: FrecII (5′-TGGTTCCGCGTGGATCTGAAAACCTGTATTTTCAGGGAGAAATTCGCGGGT-3′) and RreII (5′-GGTTTTCACCGTCATCACCGAAACGCGGAGGCAGATCGTCAGTCAGTCA-3′). The final PCR products were tagged with 50 bp matching pGEX-TEV in their 5′ and 3′ ends, respectively.

The EgFBA1 and EgEno1 open reading frames (ORFs) (1086 bp and 1299 bp, respectively) were cloned by *in vivo* homologous recombination according to Parrish et al. (2004), with minor modifications. Briefly, the vector pGEX-TEV, a version of pGEX-4-T1 (GE Healthcare) modified in our laboratory to include a cleavage site for tobacco etch virus (TEV) protease (D. M. Vargas, K. M. Monteiro, A. Zaha and H. B. Ferreira, unpublished data), was linearized with XhoI, dephosphorylated with shrimp alkaline phosphatase and purified from agarose gel using GFX Purification Kit (GE Healthcare). Vector DNA and PCR products were mixed (1:1 molar ratio) and transformed into *E. coli* KC8 cells. Transformant colonies were screened for recombinants by colony PCR, and cloned sequences were confirmed by sequencing using the Kit Dyanamic ET Dye Terminator Cycle Sequencing (GE Healthcare) in a MEGABACE 1000 Sequencing System.

2.4. Expression and purification of recombinant proteins

Recombinant protein expression and purification were carried out according to Moitinho-Silva et al. (2012), with some modifications. Briefly, recombinant plasmids carrying the *EgFBA1* and *EgEno1* ORFs were transformed into BL21-CodonPlus-RP and BL21-CodonPlus-Ril (Stratagene). Cells were grown in 1 L of CircleGrow medium (MP Bio-medicals) at 37 °C until a OD₆₀₀ of 0.8. Cultures were then induced with 0.1 mM isopropyl beta-D-1-thiogalactopyranoside (IPTG) for 5 h at 20 °C. Glutathione S-transferase (GST)-tagged recombinant proteins were purified by affinity chromatography on Glutathione Sepharose 4B (GE Healthcare) and cleaved with TEV protease for 16 h at 34 °C to be released from the GST moiety. Eluted protein concentration was measured using a Qubit™ quantitation fluorometer and Quant-it™ reagents (Invitrogen) and proper protein purification was verified by SDS-PAGE. The identity of each purified recombinant protein was confirmed by liquid chromatography–tandem mass spectrometry (LC-MS/MS), using a Waters nanoACQUITY UPLC system coupled to a Waters Micromass Q-TOF Micro mass spectrometer (Waters).

2.5. Antisera production and antibody purification

For antisera production, rabbits were immunized by subcutaneous injection with 150 µg of each recombinant protein in complete Freund's adjuvant (Sigma). Immunization was followed by two (rEgFBA1) or three (rEgEno1) boosters of 150 µg protein in incomplete Freund's adjuvant (Sigma) every three weeks. Sera titers were checked by ELISA one week after each injection using the recombinant proteins as antigens.

IgG antibody purification from non-immune control sera and from polyclonal sera from immunized animals was carried out in HiTrap Protein G HP columns (GE Healthcare), according to the manufacturer's protocol.

2.6. Immunoblots

Protein extracts from cyst components (protoscolexes, germinal layer and hydatid fluid), protoscolex tegumental fractions and ES products used in immunoblots were obtained from individual cysts and processed as described in Section 2.1. Protein samples were resolved by 12% SDS-PAGE and transferred to nitrocellulose membranes (Hybond™-ECL™, GE Healthcare) at 15 V for 30 min in a Trans-Blot SD Semi-Dry Transfer System (Bio-Rad). Membranes were processed essentially as described by Monteiro et al. (2010). Rabbit polyclonal sera anti-rEgFBA1 (diluted 1:10,000 v/v) or anti-rEgEno1 (diluted 1:5000 v/v) were used as primary antibodies, and horseradish peroxidase (HRP)-labeled anti-rabbit IgG (ECL™, GE Healthcare) was used as secondary antibody (1:9000 v/v dilution). Antigen–antibody complexes were detected using ECL detection reagent (GE Healthcare) and imaged using a VersaDoc imaging system (Bio-Rad).

2.7. Immunofluorescence

E. granulosus protoscolexes and the cyst wall tissues were fixed, dehydrated and embedded in paraffin as described by Paredes et al. (2007). Sections 5 µm thick were mounted, rehydrated, and blocked with 1% bovine serum albumin, 0.05% Tween in PBS for 1 h at 37 °C. Processed sections were then incubated in a humid chamber for 1 h at 37 °C with purified primary IgG antibodies (Section 2.5) diluted (1:50 v/v in blocking solution), followed by three washes with PBS and incubation in a humid chamber for 1 h at 37 °C with goat anti-rabbit IgG conjugated with Alexa Fluor 488 (Invitrogen) diluted (1:100 v/v in blocking solution). After three additional washes in PBS, sections were incubated with 50 mM DAPI for 20 min at 37 °C, mounted with Fluoromount and observed under the confocal

microscope (Olympus FluoView 1000). Images were digitally captured and processed using the Olympus Fluoview Ver. 2.1c and the Olympus Fluoview Ver. 3.0 Viewer softwares, respectively.

2.8. EgFBA1 modeling

A 3D molecular model of EgFBA1 was built by comparative modeling. Search for templates and generation of molecular models were conducted as described elsewhere (da Fonsêca et al., 2011). Templates used for EgFBA1 modeling were FBAs from *Drosophila melanogaster* (Hester et al., 1991) (PDB code: 1FBA), from rabbit muscle (Blom and Sygusch, 1997) (PDB code: 1ADO) and liver (PDB code: 1FDJ), and from human muscle (Dalby et al., 1999) (PDB code: 4ALD). The alignment between EgFBA1 and the templates was used to generate EgFBA 3D structure using Modeller Ver. 9.9 (Eswar et al., 2007). The final model was selected for evaluation using the following servers: PROCHECK through PDBsum (Laskowski, 2009), and PROSA-web (Wiederstein and Sippl, 2007). Visualization and manipulation of molecular images were performed with Pymol Ver. 1.2 (www.pymol.org).

2.9. Protein cross-linking and mass spectrometry for protein identification

The sulfo-succinimidyl-2-[6-(biotinamido)-2-(p-azido-benzamido) hexanoamido] ethyl-1,3-dithiopropionate (Sulfo-SBED) cross-linker (Pierce) was used for protein cross-linking experiments, according to manufacturer's instructions. Briefly, 1 mg of rEgFBA1 was labeled with a 5-fold molar excess of Sulfo-SBED and Sulfo-SBED-labeled rEgFBA1 was incubated for 30 min with a protoscolex protein extract (Section 2.1) under UV irradiation produced by a Boitton UV lamp (365 nm, 6 W) at a distance of 5 cm. Sulfo-SBED disulfide bonds from rEgFBA1–Sulfo-SBED-interacting protein complexes were cleaved with dithiothreitol and biotin-labeled proteins were recovered by affinity chromatography using a monomeric avidin column (Pierce). The recovered interacting proteins were submitted to trypsin digestion, desalted and analyzed by LC-MS/MS as described by Monteiro et al. (2010). Database searching for protein identifications was performed in local *E. granulosus* and platyhelminths EST databases and in *E. multilocularis* annotated sequences available on GeneDB, using Mascot software Ver. 2.2.1.

3. Results

3.1. Echinococcus FBA and enolase genes and encoded proteins

EST clusters for FBA (EGC00369) and enolase (EGC03002 and EGC04828, corresponding to partial 5' and 3' ORF ends, respectively), available on LophoDB Database, were initially used as search queries to recover homologous sequences in the available *E. granulosus* genome sequences. As a result, four FBA putative paralog genes and three enolase putative paralog genes were found. These FBA and enolase genes were named *EgFBA1-4* and *EgEno 1-3*. Ortholog gene sequences from *E. multilocularis*, recovered from GeneDB, were respectively named *EmFBA1-4* and *EmEno1-3*. Structure of *E. granulosus* and *E. multilocularis* FBA and enolase genes and genomic distribution of these genes in both species are shown in Table 1 and Supplementary Fig. S1 and Table S1.

E. granulosus and *E. multilocularis* orthologs for FBA (e.g. *EgFBA1* and *EmFBA1*) and enolase genes (e.g. *EgEno1* and *EmEno1*) are all well conserved in terms of both exon and intron sequences, size and relative positions, with minor differences in intron size and sequence found only between *EgFBA3* and *EmFBA3*, between *EgFBA4* and *EmFBA4* and between *EgEno3* and *EmEno3* (Table 1 and Supplementary Figs. S1, S2 and S3). Almost all predicted introns display canonical splice sites consistent with the GT-AG rule in *E. granulosus* and *E. multilocularis* FBA and enolase genes. Only three FBA introns showed non-canonical splice

Table 1Structure and characteristics of *E. granulosus* and *E. multilocularis* putative FBA and enolase genes and their encoded proteins.

Gene	Gene length ^a	ORF ^b	E 1	I 1	E 2	I 2	E 3	I 3	E 4	I 4	E 5	I 5	E 6	I 6	E 7	Protein	Length (aa)	Mass (Da)	pI
<i>EgFBA1</i>	1235	1092	540	76	259	67	293	–	–	–	–	–	–	–	–	EgFBA1 ^c	363	39666.3	8.31
<i>EmFBA1</i>	1235	1092	540	76	259	67	293	–	–	–	–	–	–	–	–	EmFBA1 ^d	363	39667.2	8.03
<i>EgFBA2</i>	1218	1095	543	34	459	89	93	–	–	–	–	–	–	–	–	EgFBA2	364	39967.7	6.27
<i>EmFBA2</i>	1218	1095	543	34	459	89	93	–	–	–	–	–	–	–	–	EmFBA2	364	39967.7	6.27
<i>EgFBA3</i>	2973	1122	327	1033	243	302	259	86	200	430	93	–	–	–	–	EgFBA3	373	41605.8	7.97
<i>EmFBA3</i>	2886	1122	327	993	243	279	259	86	200	406	93	–	–	–	–	EmFBA3	373	41373.5	7.06
<i>EgFBA4</i>	2302	1101	163	39	189	66	197	436	259	481	200	179	93	–	–	EgFBA4	380	41506.4	6.38
<i>EmFBA4</i>	2294	1101	163	33	189	66	197	436	259	479	200	179	93	–	–	EmFBA4	380	41555.5	6.57
<i>EgEno1</i>	1449	1302	310	78	635	69	357	–	–	–	–	–	–	–	–	EgEno1 ^e	433	46561.2	6.48
<i>EmEno1</i>	1449	1302	310	78	653	69	357	–	–	–	–	–	–	–	–	EmEno1	433	46560.2	6.48
<i>EgEno2</i>	1296	1296	–	–	–	–	–	–	–	–	–	–	–	–	–	EgEno2	431	46880.2	5.17
<i>EmEno2</i>	1296	1296	–	–	–	–	–	–	–	–	–	–	–	–	–	EmEno2	431	46771.1	5.16
<i>EgEno3</i>	3319	1317	85	1046	228	244	68	72	289	71	278	339	234	230	135	EgEno3	438	47676.7	6.34
<i>EmEno3</i>	3280	1317	85	1032	228	244	68	72	289	71	278	317	234	227	135	EmEno3	438	47693.8	6.19

All sequence sizes in bp. E: exon; I: intron.

^a Gene length refers to the sum of exons and introns.^b ORF length refers to the sum of exons.^c Sequence derived from EST cluster EGC00369 <http://www.nematodes.org/NeglectedGenomes/Lopho/LophDB.php>.^d EmFBA1 corresponds to the *E. multilocularis* putative fructose-bisphosphate aldolase deposited in GenBank under access number CAC18550.1.^e EgEno1 corresponds to the *E. granulosus* enolase sequence deposited in GenBank under access number GU080332.

sites GC-AG (intron 2 of *EgFBA2* and *EmFBA2*, and introns 2 and 3 of *EgFBA4* and *EmFBA4*).

EGC00369 EST cluster corresponds to *EgFBA1*, while EGC03002 and EGC04828 EST clusters correspond to *EgEno1*. No ESTs corresponding to the other *EgFBA* and *EgEno* genes have been found, and, therefore, *EgFBA1* and *EgEno1* and their protein products (*EgFBA1* and *EgEno1*, respectively) became the focus of this study. Sizes, molecular masses and isoelectric points of the proteins encoded by the *E. granulosus* and *E. multilocularis* FBA and enolase genes are presented in Table 1.

The alignment of *E. granulosus* and *E. multilocularis* FBA and enolase deduced amino acid sequences (Supplementary Fig. S4) showed high conservation between both paralog and ortholog proteins. Considering *E. granulosus* paralogs, *EgFBA1* presented 72% of amino acid identity (84% similarity) with *EgFBA2*, 51% identity (71% similarity) with *EgFBA3*, and 66% identity (76% similarity) with *EgFBA4* (Supplementary Fig. S4A), while *EgEno1* presented 74% identity (85% similarity) with *EgEno2*, and 66% identity (80% similarity) with *EgEno3* (Supplementary Fig. S4B). The alignments between the *E. granulosus* FBA and enolase deduced protein sequences with their *E. multilocularis* counterparts, in turn, showed levels of identity/similarity between 97%/97% and 100%/100% in the comparisons between the ortholog sequences of these two species. *EgFBA1* and *EgEno1* amino acid sequences were also aligned with ortholog sequences from other eukaryotes (data not shown). *EgFBA1* showed identity/similarity levels of 74%/84% to *Schistosoma mansoni* aldolase, 65%/74% to *Caenorhabditis elegans* aldolase Ce2 and 64%/76% to human aldolase A. *EgEno1*, in turn, showed identity/similarity levels of 74%/88% to *S. mansoni* enolase, 74%/87% to human enolase α , and 74%/85% to *C. elegans* enolase enol-1.

3.2. Recombinant protein expression and purification

EgFBA1 and *EgEno1* ORFs were expressed in *E. coli* as GST-tagged proteins. *E. coli* strains BL21-CodonPlus-RP and BL21-CodonPlus-RIL were tested as hosts, with the first being more suitable for r*EgFBA1* expression, and the second for r*EgEno1* expression (Supplementary Fig. S5). Attempts to express these proteins at 37 °C resulted in reduced solubility (data not shown) and, therefore, protein expression was carried out at 20 °C. Purified r*EgFBA1* and r*EgEno1* presented the expected molecular masses of 39.6 and 46.5 kDa, respectively. About 4 mg of r*EgFBA1* and 3 mg of r*EgEno1* per liter of culture were obtained. The identity of these proteins was confirmed by LC-MS/MS mass spectrometry analysis (data not shown).

3.3. *EgFBA1* and *EgEno1* detection in hydatid cyst components

Rabbit monospecific polyclonal antibodies against *EgFBA1* and *EgEno1* were used in immunoblot experiments to probe samples from different metacestode components. Based on the *E. granulosus* transcriptomic and proteomic data (LophDB database and Monteiro et al., 2010, respectively) *EgFBA1* and *EgEno1* were assumed as the only detectable *EgFBA* and *EgEno* isoforms in the metacestode. This assumption is also corroborated by *E. multilocularis* RNAseq data (Wellcome Trust Sanger Institute, unpublished data), which indicate that *EgFBA1* and *EgEno1* orthologs (*EmFBA1* and *EmEno1*, respectively) correspond to the predominantly expressed isoforms in the metacestode stage.

In the *E. granulosus* metacestode, *EgFBA1* and *EgEno1* presence was demonstrated in protoscoleces, in the germinal layer, and in the hydatid fluid as bands corresponding to the expected molecular masses (of 39.6 and 46.5 kDa, respectively) (Fig. 1). Immunofluorescence assays were used to refine this result in protoscoleces and in the cyst wall, showing that these proteins are widely distributed in all tissues, with confirmation of their expected cytoplasmic localization (Figs. 2D and H, middle and lower panels). Differential expression of *EgFBA1* and *EgEno1* in the cyst wall was also revealed by immunofluorescence labeling. Although the localization of both proteins in the germinal layer is quite similar (Fig. 2H, middle and lower panel), *EgEno1*, but not *EgFBA1*, was detected in the laminated layer (Fig. 2H, lower panel), which separates the cyst germinal layer from the surrounded host-produced adventitial layer.

To further investigate the presence of *EgFBA1* and *EgEno1* in parasite's host-interacting components we also analyzed protoscoleces tegument fractions and ES products (Fig. 3). Both *EgFBA1* and *EgEno1* were found in different tegumental fractions (Fig. 3A). Their detection in protein fractions extracted with urea is indicative of their association to cytoskeletal components. Likewise, the detection of *EgEno1* as a faint band in the protein fractions extracted with SDS/Triton X-100 suggests that this protein has some degree of surface association. Additionally, these enzymes were detected as ES products from protoscoleces in culture (Fig. 3B). Overall, these results are indicative that these enzymes are distributed in important host-interaction components.

3.4. *EgFBA1* modeling

In the attempt to find structural features that could be indicative of moonlighting functions, we have modeled *EgFBA1*. To generate

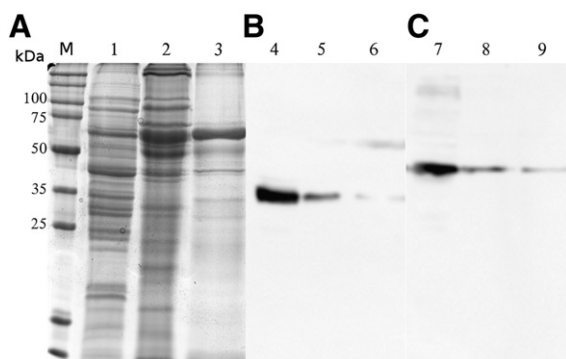


Fig. 1. Detection of EgFBA1 and EgEno1 in *E. granulosus* hydatid cyst components. (A) Parasite protein extracts resolved by 12% SDS-PAGE and stained with Coomassie R-250. Immunoblots were probed with polyclonal serum against EgFBA1 (B) and EgEno1 (C). Molecular mass markers are indicated (kDa). All lanes were loaded with 40 µg of protein. Lanes 1, 4 and 7: protoscolex extract; lanes 2, 5 and 8: germinal layer extract; lanes 3, 6 and 9: hydatid fluid.

an EgFBA1 3D model, templates with identities ranging from 63% (1FDJ) to 67% (1FBA) were used, and these high identity levels allowed the construction of a model with high confidence. The obtained structure presented a $(\alpha/\beta)_8$ barrel fold architecture (Fig. 4), consistent with those of its templates. The hydrogen bonding between the phosphate groups of the fructose 1,6-bisphosphate (Fru 1,6-P2) substrate to FBA involves the following amino acids Asp34, Ser36, Ser38, Lys108, Lys147, Arg149, Glu188, Glu190, Lys230, Ser272, Arg304 and Leu357 (Dalby et al., 1999), all conserved in EgFBA1. Besides the binding site for Fru 1,6-P2, EgFBA1 also appears to possess a F-actin binding site, since five amino acids previously confirmed to be involved in such interaction (Asp34, Arg43, Lys108, Arg149 and Lys230; Wang et al., 1996) are conserved. Except for Arg43, all these amino acids are also involved in Fru 1,6-P2 binding (see above). Ramachandran plotting showed that in the structure 99% of the EgFBA1 model amino acids lie in favored and additional allowed regions. ProSA-web was used to test for overall model quality and provided a z-score of -10.42 , which falls within the range of values observed for experimentally determined structures of similar lengths.

3.5. Confirmation of predicted EgFBA1 interactions with other proteins

To functionally investigate the EgFBA1 binding properties, we have performed an *in vitro* protein–protein cross-linking interaction assay, using Sulfo-SBED. Mass spectrometry analysis of EgFBA1-interacting proteins recovered from protoscolex extracts allowed the identification of 3 proteins (Table 2). The actin identification indicates the functionality of the *in silico* predicted EgFBA1 actin-binding site (see Section 3.4).

4. Discussion

The glycolytic pathway and its enzymes, which convert glucose to pyruvic acid using the oxidative potential of NAD^+ , are among the most ancient molecular metabolic networks (Canback et al., 2002). Several reports have shown that these enzymes perform a number of functions in addition to their innate glycolytic function and play important roles in several biological and pathophysiological processes (Kim and Dang, 2005; Sirover, 1999; Sriram et al., 2005). FBA and

enolase are examples of multifunctional proteins and they have been described performing moonlighting functions in different biological contexts, including parasitism (Ramajo-Hernández et al., 2007; Tunio et al., 2010).

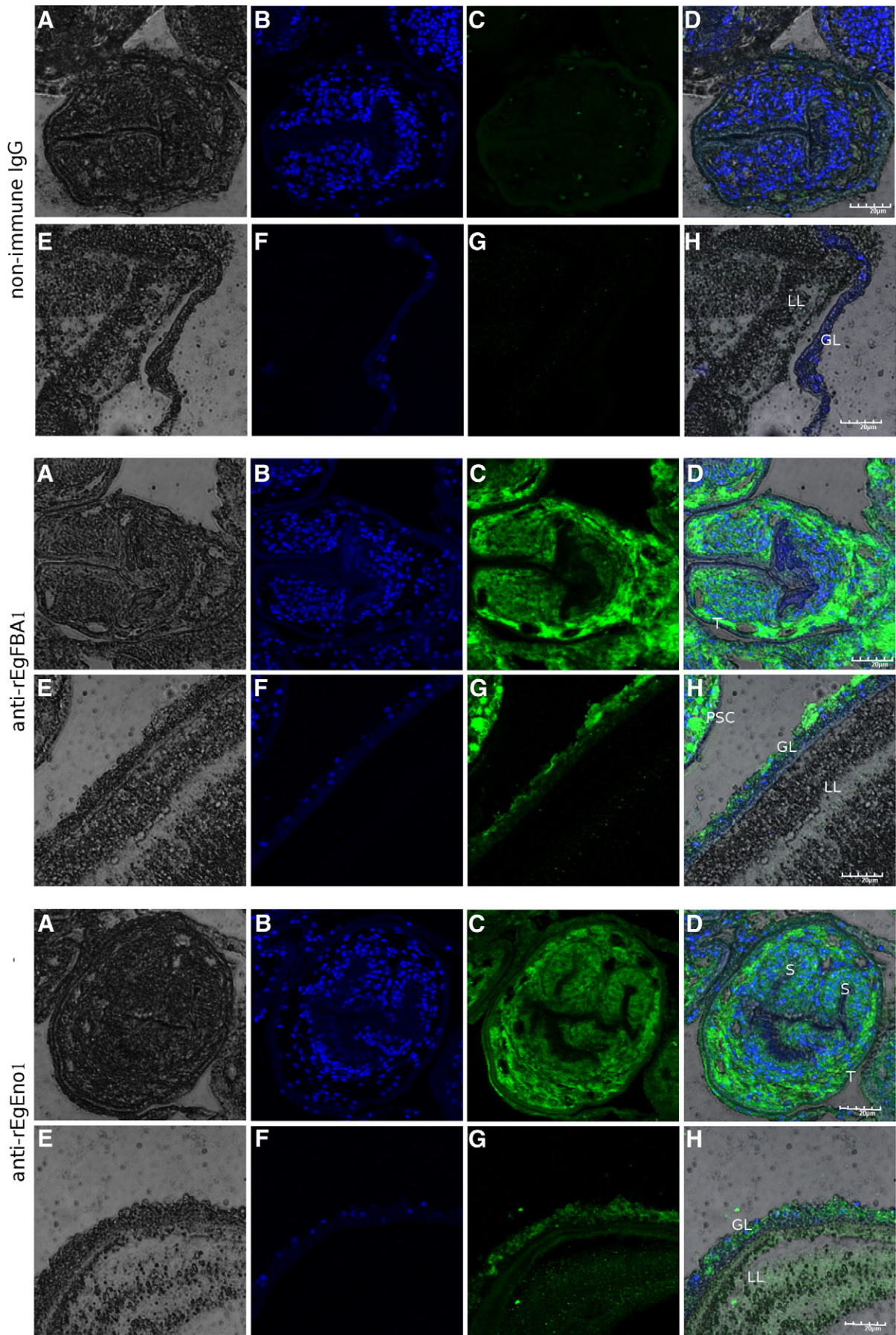
Aldolase primary function is the catalysis of the reversible cleavage of Fru 1,6-P2 to dihydroxyacetone phosphate and glyceraldehyde 3-phosphate. Its functional form is either homo- or hetero-tetrameric. Evidence for EgFBA1 oligomerization was provided by our protein cross-linking assay, which identified this enzyme isoform as one of its ligands. In vertebrates, there are three isozymes (encoded by different genes) that have different activities and vary in their tissue distribution: aldolase A (predominantly present in muscle), aldolase B (in liver) and aldolase C (in brain) (Kukita et al., 1988; Shiokawa et al., 2002). In invertebrates, the presence of more than one aldolase isoform has also been described. In *D. melanogaster* there are three isozymic forms of aldolase which are generated from a single gene by alternative splicing (Kai et al., 1992). *C. elegans* and *Clonorchis sinensis* present two and three isozymes, respectively (Cho et al., 2006; Inoue et al., 1997), and similarly to vertebrates, each of these isozymes is encoded by different genes.

Enolase primary function is the catalysis of the reversible transformation between 2-phospho-glyceric acid and phosphoenolpyruvic acid. In vertebrates, there are three genes encoding three enolase isoenzymes (α , β and γ), which usually function as homodimers and are expressed in different tissues (McAleese et al., 1988). In invertebrates, there are evidences for the presence of more than one enolase gene with differential regulation. For instance, two enolase genes have been reported for the silkworm *Antheraea pernyi* (Liu et al., 2010) and for *Toxoplasma gondii* (Dziersinski et al., 2001). In *S. japonicum*, southern blot analysis suggested that this parasite also contains more than one enolase gene (Waine et al., 1993).

In *E. granulosus*, our *in silico* analysis indicates the presence of four FBA genes and three enolase genes. EgFBA2, EgFBA3, EgFBA4, EgEno2 and EgEno3 are here being reported for the first time, since previous transcriptional (Fernández et al., 2002) and proteomic (Monteiro et al., 2010) studies of hydatid cyst samples have only detected EgFBA1 and EgEno1 products, and no genomic surveys for *E. granulosus* FBA and enolase encoding genes have been conducted so far. EgFBA2–4 and EgEno2–3 are structurally integrous, at least regarding their exon–intron structures, and, therefore, are likely functional, assuming that previous failing in the detection of their RNA or protein products could be explained by their possible expression solely or preferentially in stages other than the larval stage, in which only EgFBA1 and EgEno1 products were detected. Further studies with *E. granulosus* oncospheres or adult worms will be necessary to address this issue, and, for the moment, only EgFBA1 and EgEno1, expressed in the parasite's pathogenic larval form, including the host interface, will be further discussed here.

As a first approach to gather evidence of possible moonlighting functions for EgFBA1 and EgEno1, we immunolocalized these proteins in components of the parasite larval stage. The used antibodies were produced against recombinant versions of EgFBA1 and EgEno1, the only EgFBA and EgEno isoforms whose expression was so far detected in *E. granulosus* metacystode material (Fernández et al., 2002; Monteiro et al., 2010). In the cyst wall, the distribution of EgEno1 calls attention due to its presence not only in germinal layer, but also in laminated layer. The laminated layer is an acellular, carbohydrate-rich sheath secreted by the germinal layer, and was evolutionarily designed for maintaining the physical integrity of metacystodes and for protecting germinal layer cells from host

Fig. 2. Immunolocalization of EgFBA1 and EgEno1 in *E. granulosus* protoscolexes (A–D) and cyst wall (E–H). Parasite sections (5 µm) were incubated with purified non-immune IgG (1:50 v/v) (upper panel), purified IgG anti-rEgFBA1 (1:50 v/v) (middle panel) and purified IgG anti-rEgEno1 (1:50 v/v) (lower panel). Recognition of immune complexes was achieved using Alexa 488-conjugated secondary antibodies. A and E: bright field images; B and F: DAPI nuclei staining; C and G: antibody staining; D and H: bright field merges of DAPI and antibody staining. GL: germinal layer; LL: laminated layer; PSC: protoscolex; S: sucker; T: tegument. Scale bar: 20 µm.



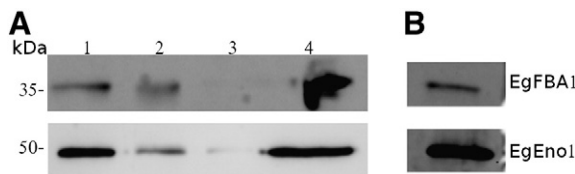


Fig. 3. Detection of EgFBA1 and EgEno1 in protoscolex tegument and ES products. Immunoblots were probed with polyclonal serum against EgFBA1 or EgEno1, as indicated. (A) Immunoblots of tegumental proteins extracted according to their solubility (20 µg of protein/lane). Lanes 1, 2 and 3: tegumental fractions extracted with 40 mM Tris, 5 M urea and 0.1% SDS/1% Triton X-100, respectively; lane 4: non-tegumental fraction. (B) Immunoblots of culture supernatants containing protoscolex *in vitro* ES products (1 µg protein/lane). Molecular masses are indicated on the left side of the figure.

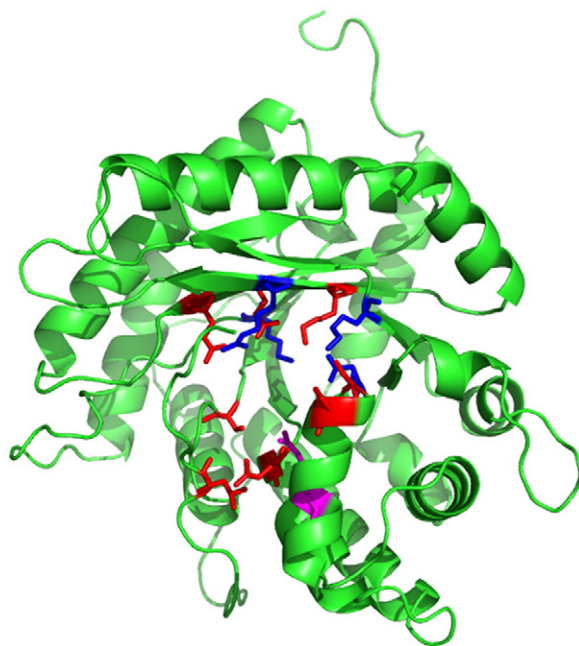


Fig. 4. 3D structure of EgFBA1. Highlighted in green are α -helices, β -sheet and loops. Amino acids involved in Fru 1,6-P2 binding (Asp34, Ser36, Ser38, Lys108, Lys147, Arg149, Glu188, Glu190, Lys230, Ser272, Arg304 and Leu357) are shown in red; amino acids proposed to interact with F-actin (Asp34, Arg43, Lys108, Arg149 and Lys230) are shown in magenta; and amino acids involved in interactions with both Fru 1,6-P2 and actin (Asp34, Lys108, Arg149 and Lys230) are shown in blue. (For interpretation of the references to color in this figure legend, the reader is referred to the web version of this article.)

immunity (Díaz et al., 2011). Therefore, the detection of EgEno1 in the laminated layer is indicative of its direct involvement with survival mechanisms in the parasite–host interface.

In protoscolexes, immunostaining revealed a wide distribution of both EgFBA1 and EgEno1, which is compatible with their primary function as glycolytic enzymes in the cytoplasm. However, in addition to EgEno1 cytoplasmic localization, its detection in the protoscolex tegumental fraction extracted with detergent confirms its association with surface membranes. It is known that proteins that are expressed or secreted on the surface of pathogens are potential players in host–parasite molecular crosstalk (Vivona et al., 2008). Although protoscolexes are not directly exposed to the intermediate host in the hydatid cyst, their surface proteins are accessible to interaction with host molecules that permeate the cyst and can become directly accessible for interactions with host tissues upon cyst rupture and consequent cyst content leakage. In this later scenario, protoscolex tegumental proteins are assumed to be important for the recognition of host molecules and mediate the activation of signaling pathways

Table 2

Proteins identified as EgFBA1-binding in the cross-linking assay by searches in *E. granulosus* and *E. multilocularis* databases.^a

Protein	Accession number	Organism	MASCOT score ^b	Sequence coverage (%)
1 Actin	AAC37175	<i>E. granulosus</i>	23	2
	EmW_000061200	<i>E. multilocularis</i>	29	4
2 Fructose-bisphosphate aldolase	EGC00369	<i>E. granulosus</i>	106	25
	EmW_000905600	<i>E. multilocularis</i>	103	15
3 Phosphoenolpyruvate carboxykinase	EGC04068	<i>E. granulosus</i>	33	14
	EGC04111	<i>E. granulosus</i>	29	7
	EmW_000292700	<i>E. multilocularis</i>	37	7

^a Searches were performed in local *E. granulosus* and platyhelminths EST databases and in *E. multilocularis* annotated sequences available on GeneDB database.

^b MASCOT score is $-10 \times \log(P)$, where P is the probability that the observed match a random event. Individual scores >22 indicate identity or extensive homology for $p \leq 0.05$.

involved in dedifferentiation of protoscolexes into secondary hydatid cysts (Breijo et al., 1998). Similarly, upon ingestion by the definitive host, tegumental proteins are likely to be important for protoscolex fixation in the small intestine and differentiation into the adult worm. Therefore, the EgEno1 presence at parasite surface favors the interaction with host tissues and molecules, and might have important non-glycolytic functions in these different contexts.

Although mechanisms regulating the presence of the EgEno1 in protoscolex tegument surface are still unknown, this location is evocative of moonlighting functions. Enolase has been found in the tegument of adult *Schistosoma* and *Opisthorchis* worms (Mulvenna et al., 2010a, 2010b), suggesting that this enzyme location in the adult stage could be usual in parasitic flatworms. Another possibility, not mutually exclusive, is that different localizations could be regulated by the presence of substrates. In situations of high metabolic activities, EgFBA1 and EgEno1 would be especially needed in the cytoplasm, but, in situations of reduced metabolic activity, they could be directed to other locations and used for other functions (Tovy et al., 2010). Regarding parasite evolution, this kind of enzyme multifunctionality may have contributed in some degree for biological streamlining associated with adaptation to parasitism (Collingridge et al., 2010).

Equally noticeable is the presence of both EgFBA1 and EgEno1 in ES products. Both proteins have already been identified by proteomic analyses of *E. granulosus* hydatid fluid (Aziz et al., 2011; Monteiro et al., 2010) and *in vitro* ES products of protoscolexes (Virginio et al., 2012). Here, these proteins were detected accordingly, both in the hydatid fluid (containing ES products of the germinal layer and protoscolex) and in the ES products from *in vitro* cultures of protoscolexes. The absence of a typical leader peptide sequence in N-terminal end of EgFBA1 and EgEno1 excludes the involvement of the classical secretory pathway for surface transport. Therefore, the presence of these glycolytic enzymes in the ES products could be explained either by parasite tegument shedding or by a so far unknown transport mechanism. On the other hand, to access whether the parasite/host pair is determinant in the presence of cytoplasmic proteins in the hydatid fluid, other parasite/host combination (G5/cattle and G1/sheep) will be addressed in future studies.

The presence of glycolytic enzymes in the ES products has been previously described in many helminth parasites (Bernal et al., 2004; Guillou et al., 2007; Marcilla et al., 2007; Stadelmann et al., 2010; Wang et al., 2011) and is, therefore, unlikely to have occurred by chance. For example, the presence of *E. multilocularis* phosphoglucose isomerase in the vesicle fluid seems to be related to cellular proliferation and/or differentiation of the germinal layer-associated tissue (Stadelmann et al., 2010). In *C. sinensis*, the inhibition of the enolase in the ES products affects the parasite growth (Wang et al., 2011). Although the exact mechanism responsible for releasing of

these glycolytic enzymes remains a challenging question, the relevance of this process is evident.

Besides EgFBA1 and EgEno1 localization, some structural features additionally support multifunctionality of these proteins. The EgFBA1 conserved F-actin binding site, modeled and experimentally confirmed here, is suggestive of interactions with the cytoskeleton, which is consistent with our protein–protein interaction result where the actin was identified as one of the EgFBA1 partner proteins. The actin binding ability of aldolase has been shown in previous studies for both non-parasite (Wang et al., 1996) and parasite organisms (Starnes et al., 2009), and, in apicomplexan parasites, aldolase was described as a member of a multiprotein complex connecting adhesins to cytoskeleton, providing a model linking adhesion to motility (Jewett and Sibley, 2003; Starnes et al., 2009). For EgEno1, a structural study (Gan et al., 2010) predicted a transmembrane domain. Accordingly, this protein is extracted from the tegumental fraction with detergent. Enolase surface localization has also been described for several parasites, favoring the interaction of enolase with host proteins, like plasminogen (de la Torre-Escudero et al., 2010).

In conclusion, the results presented here showed that, in both *E. granulosus* and *E. multilocularis*, four FBA isoforms and three enolase isoforms were predicted. In *E. granulosus*, only one EgFBA and one EgEno isoform were detected in the pathogenic larval form. EgFBA1 and EgEno1 expression patterns in hydatid cyst components showed that these proteins are exposed in the host–parasite interface, raising evidence of their involvement in molecular signaling pathways important for parasite survival and development. The EgFBA1–actin binding property and EgEno1 surface association, along with their presence in parasite ES products, are indicative of non-glycolytic functions in the host–parasite interplay. We are currently investigating the EgFBA1 and EgEno1 protein interaction networks, in order to understand how the multifunctionality of these glycolytic enzymes is connected to parasite's biology.

Supplementary data to this article can be found online at <http://dx.doi.org/10.1016/j.gene.2012.06.046>.

Acknowledgments

We thank Dr. Magdalena Zarowiecki (Parasite Genomics Group, Wellcome Trust Sanger Institute), for information on annotation, structure and expression of *E. multilocularis* FBA and enolase genes; Centro de Microscopia Eletrônica (UFRGS), for technical support with the confocal microscopy and Uniprote-MS (Cbiot/UFRGS), for support in LC-MS/MS analyses. This work was supported by Conselho Nacional de Desenvolvimento Científico e Tecnológico (CNPq) (Convênio Bilateral de Cooperação Internacional CNPq/CONICYT), and Coordenação de Aperfeiçoamento de Pessoal de Nível Superior (CAPES) (AUX-PE-PARASITOLOGIA – 1278/2011), in Brazil, and by project DI 56-06/R (Universidad Andrés Bello), project ACT112-CONICYT (to N.G.) and FONDECYT, in Chile. K. R. L. is a recipient of a CNPq doctoral fellowship. K. M. M. is recipient of CAPES postdoctoral fellowship. G. P. P. is recipient of a CNPq graduate fellowship.

References

- Aziz, A., Zhang, W., Li, J., Loukas, A., McManus, D.P., Mulvanny, J., 2011. Proteomic characterization of *Echinococcus granulosus* hydatid cyst fluid from sheep, cattle and humans. *J. Proteomics* 74, 1560–1572.
- Bernal, D., de la Rubia, J.E., Carrasco-Abad, A.M., Toledo, R., Mas-Coma, S., Marcilla, A., 2004. Identification of enolase as a plasminogen-binding protein in excretory–secretory products of *Fasciola hepatica*. *FEBS Lett.* 563, 203–206.
- Blom, N., Sygusch, J., 1997. Product binding and role of the C-terminal region in class I D-fructose 1, 6-bisphosphate aldolase. *Nat. Struct. Biol.* 4, 36–39.
- Bowles, J., Blair, D., McManus, D.P., 1992. Genetic variants within the genus *Echinococcus* identified by mitochondrial DNA sequencing. *Mol. Biochem. Parasitol.* 54, 165–173.
- Breijo, M., Spinelli, P., Sim, R., Ferreira, A.M., 1998. *Echinococcus granulosus*: an intraperitoneal diffusion chamber model of secondary infection in mice. *Exp. Parasitol.* 90, 270–276.
- Budke, C.M., Deplazes, P., Torgerson, P.R., 2006. Global socioeconomic impact of cystic echinococcosis. *Emerg. Infect. Dis.* 12, 296–303.
- Burge, C.B., Karlin, S., 1998. Finding the genes in genomic DNA. *Curr. Opin. Struct. Biol.* 8, 346–354.
- Canback, B., Andersson, S.G.E., Kurland, C.G., 2002. The global phylogeny of glycolytic enzymes. *Proc. Natl. Acad. Sci. U. S. A.* 99, 6097–6102.
- Carmena, D., Benito, A., Eraso, E., 2006. Antigens for the immunodiagnosis of *Echinococcus granulosus* infection: an update. *Acta Trop.* 98, 74–86.
- Chemale, G., et al., 2003. Proteomic analysis of the larval stage of the parasite *Echinococcus granulosus*: causative agent of cystic hydatid disease. *Proteomics* 3, 1633–1636.
- Cho, P.Y., Lee, M.J., Kim, T.I., Kang, S.Y., Hong, S.J., 2006. Expressed sequence tag analysis of adult *Clonorchis sinensis*, the Chinese liver fluke. *Parasitol. Res.* 99, 602–608.
- Collingridge, P.W., Brown, R.W.B., Ginger, M.L., 2010. Moonlighting enzymes in parasitic protozoa. *Parasitology* 137, 1467–1475.
- da Fonseca, M.M., Zaha, A., Caffarena, E.R., Vasconcelos, A.T.R., 2011. Structure-based functional inference of hypothetical proteins from *Mycoplasma hyopneumoniae*. *J. Mol. Model.* 17, 1–9.
- Dalby, A., Dauter, Z., Littlechild, J.A., 1999. Crystal structure of human muscle aldolase complexed with fructose 1,6-bisphosphate: mechanistic implications. *Protein Sci.* 8, 291–297.
- de la Torre-Escudero, E., Manzano-Román, R., Pérez-Sánchez, R., Siles-Lucas, M., Oleaga, A., 2010. Cloning and characterization of a plasminogen-binding surface-associated enolase from *Schistosoma bovis*. *Vet. Parasitol.* 173, 76–84.
- Díaz, A., Casaravilla, C., Allen, J.E., Sim, R.B., Ferreira, A.M., 2011. Understanding the laminated layer of larval *Echinococcus* II: immunology. *Trends Parasitol.* 27, 264–273.
- Dziarsinski, F., Mortuaire, M., Dendouga, N., Popescu, O., Tomavo, S., 2001. Differential expression of two plant-like enolases with distinct enzymatic and antigenic properties during stage conversion of the protozoan parasite *Toxoplasma gondii*. *J. Mol. Biol.* 309, 1017–1027.
- Eswar, N., et al., 2007. Comparative protein structure modeling using MODELLER. *Curr. Protoc. Protein Sci.* 50, 2.9.1–2.9.31.
- Fernández, C., Gregory, W.F., Loke, P., Maizels, R.M., 2002. Full-length-enriched cDNA libraries from *Echinococcus granulosus* contain separate populations of oligo-capped and trans-spliced transcripts and a high level of predicted signal peptide sequences. *Mol. Biochem. Parasitol.* 122, 171–180.
- Gan, W., et al., 2010. Reverse vaccinology approach identify an *Echinococcus granulosus* tegumental membrane protein enolase as vaccine candidate. *Parasitol. Res.* 106, 873–882.
- Gancedo, C., Flores, C.L., 2008. Moonlighting proteins in yeasts. *Microbiol. Mol. Biol. Rev.* 72, 197–210.
- Guillou, F., et al., 2007. Excretory–secretory proteome of larval *Schistosoma mansoni* and *Echinostoma caproni*, two parasites of *Biomphalaria glabrata*. *Mol. Biochem. Parasitol.* 155, 45–56.
- Haile, W.B., Coleman, J.L., Benach, J.L., 2006. Reciprocal upregulation of urokinase plasminogen activator and its inhibitor, PAI-2, by *Borrelia burgdorferi* affects bacterial penetration and host-inflammatory response. *Cell. Microbiol.* 8, 1349–1360.
- Hester, G., et al., 1991. The crystal structure of fructose-1,6-bisphosphate aldolase from *Drosophila melanogaster* at 2.5 Å resolution. *FEBS Lett.* 292, 237–242.
- Huang, J., Huang, Y., Wu, X., Du, W., Yu, X., Hu, X., 2009. Identification, expression, characterization, and immunolocalization of lactate dehydrogenase from *Taenia asiatica*. *Parasitol. Res.* 104, 287–293.
- Huberts, D.H.E.W., Van Der Klei, I.J., 2010. Moonlighting proteins: an intriguing mode of multitasking. *Biochim. Biophys. Acta* 1803, 520–525.
- Inoue, T., et al., 1997. *Caenorhabditis elegans* has two isozymic forms, CE-1 and CE-2, of fructose-1,6-bisphosphate aldolase which are encoded by different genes. *Arch. Biochem. Biophys.* 339, 226–234.
- Jeffery, C., 1999. Moonlighting proteins. *TIBS* 24, 8–11.
- Jewett, T.J., Sibley, L.D., 2003. Aldolase forms a bridge between cell surface adhesins and the actin cytoskeleton in apicomplexan parasites. *Mol. Cell* 11, 885–894.
- Kai, T., Sugimoto, Y., Kusakabe, T., Zhang, R., Koga, K., Hori, K., 1992. Gene structure and multiple mRNA species of *Drosophila melanogaster* aldolase generating three isozymes with different enzymatic properties. *J. Biochem.* 112, 677–688.
- Kim, J.W., Dang, C.V., 2005. Multifaceted roles of glycolytic enzymes. *Trends Biochem. Sci.* 30, 142–150.
- Kukita, A., Mukai, T., Miyata, T., Hori, K., 1988. The structure of brain-specific rat aldolase C mRNA and the evolution of aldolase isozyme genes. *Eur. J. Biochem.* 171, 471–478.
- Labbé, M., Péroval, M., Bourdieu, C., Girard-Misguich, F., Péry, P., 2006. *Eimeria tenella* enolase and pyruvate kinase: a likely role in glycolysis and in others functions. *Int. J. Parasitol.* 36, 1443–1452.
- Larkin, M.A., et al., 2007. Clustal W and Clustal X version 2.0. *Bioinformatics* 23, 2947–2948.
- Laskowski, R.A., 2009. PDBsum new things. *Nucleic Acids Res.* 37, D355–D359.
- Liu, Y., et al., 2010. cDNA cloning and expression pattern of two enolase genes from the Chinese oak silkworm, *Antheraea pernyi*. *Acta Biochim. Biophys. Sin.* 42, 816–826.
- Logan-Klumpler, F.J., et al., 2012. GeneDB—an annotation database for pathogens. *Nucleic Acids Res.* 40, D98–D108.
- Lomsadze, A., Ter-Hovhannisyan, V., Chernoff, Y., Borodovsky, M., 2005. Gene identification in novel eukaryotic genomes by self-training algorithm. *Nucleic Acids Res.* 33, 6494–6506.
- Marcilla, A., et al., 2007. *Echinostoma caproni*: identification of enolase in excretory/secretory products, molecular cloning, and functional expression. *Exp. Parasitol.* 117, 57–64.
- McAleese, S.M., Dunbar, B., Fothergill, J.E., Hinks, L.J., Day, I.N., 1988. Complete amino acid sequence of the neurone-specific gamma isozyme of enolase (NSE) from human brain and comparison with the non-neuronal alpha form (NNE). *Eur. J. Biochem.* 178, 413–417.
- McCarthy, J.S., et al., 2002. *Onchocerca volvulus* glycolytic enzyme fructose-1, 6-bisphosphate aldolase as a target for a protective immune response in humans. *Infect. Immun.* 70, 851–858.

- Moitinho-Silva, L., et al., 2012. *Mycoplasma hyopneumoniae* type I signal peptidase: expression and evaluation of its diagnostic potential. *Vet. Microbiol.* 154, 282–291.
- Monteiro, K.M., de Carvalho, M.O., Zaha, A., Ferreira, H.B., 2010. Proteomic analysis of the *Echinococcus granulosus* metacestode during infection of its intermediate host. *Proteomics* 10, 1985–1999.
- Moro, P., Schantz, P.M., 2009. Echinococcosis: a review. *Int. J. Infect. Dis.* 13, 125–133.
- Mulvenna, J., et al., 2010a. Exposed proteins of the *Schistosoma japonicum* tegument. *Int. J. Parasitol.* 40, 543–554.
- Mulvenna, J., et al., 2010b. The secreted and surface proteomes of the adult stage of the carcinogenic human liver fluke *Opisthorchis viverrini*. *Proteomics* 10, 1063–1078.
- Nicholas, K.B., Nicholas, H.B., 1997. GeneDoc: A Tool for Editing and Annotating Multiple Sequence Alignments. Distributed by the Author.
- Nogueira, S.V., et al., 2010. *Paracoccidioides brasiliensis* enolase is a surface protein that binds plasminogen and mediates interaction of yeast forms with host cells. *Infect. Immun.* 78, 4040–4050.
- Pal-Bhowmick, I., Vora, H.K., Jarori, G.K., 2007. Sub-cellular localization and post-translational modifications of the *Plasmodium yoelii* enolase suggest moonlighting functions. *Malar. J.* 6, 45.
- Paredes, R., Jiménez, V., Cabrera, G., Iragüen, D., Galanti, N., 2007. Apoptosis as a possible mechanism of infertility in *Echinococcus granulosus* hydatid cysts. *J. Cell. Biochem.* 100, 1200–1209.
- Parrish, J.R., Limjindaporn, T., Hines, J.A., Liu, J., Liu, G., Finley, R.L., 2004. High-throughput cloning of *Campylobacter jejuni* ORFs by *in vivo* recombination in *Escherichia coli*. *J. Proteome Res.* 3, 582–586.
- Pomel, S., Luk, F.C.Y., Beckers, C.J.M., 2008. Host cell egress and invasion induce marked relocations of glycolytic enzymes in *Toxoplasma gondii* tachyzoites. *PLoS Pathog.* 4, e1000188.
- Ramajo-Hernández, A., Pérez-Sánchez, R., Ramajo-Martin, V., Oleaga, A., 2007. *Schistosoma bovis*: plasminogen binding in adults and the identification of plasminogen-binding proteins from the worm tegument. *Exp. Parasitol.* 115, 83–91.
- Roberts, S., MacGregor, A., Vojvodic, M., Wells, E., Crabtree, J., Wilson, R., 1983. Tegument surface membranes of adult *Schistosoma mansoni*: development of a method for their isolation. *Mol. Biochem. Parasitol.* 9, 105–127.
- Rodrigues, J.J., Ferreira, H.B., Zaha, A., 1993. Molecular cloning and characterization of an *Echinococcus granulosus* cDNA encoding malate dehydrogenase. *Mol. Biochem. Parasitol.* 60, 157–160.
- Salamov, A.A., Solovyev, V.V., 2000. *Ab initio* gene finding in *Drosophila* genomic DNA. *Genome Res.* 10, 516–522.
- Shiokawa, K., Kajita, E., Hara, H., Yatsuki, H., Hori, K., 2002. A developmental biological study of aldolase gene expression in *Xenopus laevis*. *Cell Res.* 12, 85–96.
- Sievers, F., et al., 2011. Fast, scalable generation of high-quality protein multiple sequence alignments using Clustal Omega. *Mol. Syst. Biol.* 7, 539.
- Siracusano, A., et al., 2008. Immunomodulatory mechanisms during *Echinococcus granulosus* infection. *Exp. Parasitol.* 119, 483–489.
- Sirover, M.A., 1999. New insights into an old protein: the functional diversity of mammalian glyceraldehyde-3-phosphate dehydrogenase. *Biochim. Biophys. Acta* 1432, 159–184.
- Sriram, G., Martinez, J.A., McCabe, E.R.B., Liao, J.C., Dipple, K.M., 2005. Single-gene disorders: what role could moonlighting enzymes play? *Am. J. Hum. Genet.* 76, 911–924.
- Stadelmann, B., et al., 2010. *Echinococcus multilocularis* phosphoglucose isomerase (EmPGI): a glycolytic enzyme involved in metacestode growth and parasite–host cell interactions. *Int. J. Parasitol.* 40, 1563–1574.
- Starnes, G.L., Coincon, M., Sygusch, J., Sibley, L.D., 2009. Aldolase is essential for energy production and bridging adhesin–actin cytoskeletal interactions during parasite invasion of host cells. *Cell Host Microbe* 5, 353–364.
- Tovy, A., Siman Tov, R., Gaentzsch, R., Helm, M., Ankri, S., 2010. A new nuclear function of the *Entamoeba histolytica* glycolytic enzyme enolase: the metabolic regulation of cytosine-5 methyltransferase 2 (Dnmt2) activity. *PLoS Pathog.* 6, e1000775.
- Tunio, S.A., Oldfield, N.J., Berry, A., Ala'Aldeen, D.A.A., Wooldridge, K.G., Turner, D.P.J., 2010. The moonlighting protein fructose-1, 6-bisphosphate aldolase of *Neisseria meningitidis*: surface localization and role in host cell adhesion. *Mol. Microbiol.* 76, 605–615.
- Virginio, V.G., et al., 2012. Excretory/secretory products from *in vitro*-cultured *Echinococcus granulosus* protoscoleces. *Mol. Biochem. Parasitol.* 183, 15–22.
- Vivona, S., et al., 2008. Computer-aided biotechnology: from immuno-informatics to reverse vaccinology. *Trends Biotechnol.* 26, 190–200.
- Waine, G.J., Becker, M., Kalinna, B., Yang, W., McManus, D.P., 1993. Cloning and functional expression of a *Schistosoma japonicum* cDNA homologous to the enolase gene family. *Biochem. Biophys. Res. Commun.* 195, 1211–1217.
- Wang, J., Morris, A.J., Tolan, D.R., Pagliaro, L., 1996. The molecular nature of the F-actin binding activity of aldolase revealed with site-directed mutants. *J. Biol. Chem.* 271, 6861–6865.
- Wang, X., et al., 2011. *Clonorchis sinensis* enolase: identification and biochemical characterization of a glycolytic enzyme from excretory/secretory products. *Mol. Biochem. Parasitol.* 177, 135–142.
- Wiederstein, M., Sippl, M.J., 2007. ProSA-web: interactive web service for the recognition of errors in three-dimensional structures of proteins. *Nucleic Acids Res.* 35, 407–410.
- Zhang, W., McManus, D.P., 2006. Recent advances in the immunology and diagnosis of echinococcosis. *FEMS Immunol. Med. Microbiol.* 47, 24–41.